Inorganica Chimica Acta 524 (2021) 120438

Contents lists available at ScienceDirect

Inorganica Chimica Acta

journal homepage: www.elsevier.com/locate/ica

Research paper

# A novel ratiometric fluorescent probe for sensitive and selective detection of $Cu^{2+}$ based on Boranil derivatives

Dongjian Zhu [a,*], Shilei Jiang [b], Wei Zhao [c], Xiaowei Yan [a], Wei Xie [a], Yuhao Xiong [a], Sujuan Wang [a], Wen Cai [a], Youjun Gao [d], Aishan Ren [a,*]

[a] Research Institute of Food Science and Engineering Technology, College of Food and Bioengineering, Hezhou University, Hezhou 542899, PR China
[b] Yiwu Inspection and Quarantine Academy of Science and Technology, Yiwu 322000, PR China
[c] Key Laboratory of Cluster Science of Ministry of Education, Key Laboratory of Medical Molecule Science and Pharmaceutics Engineering, Ministry of Industry and Information Technology, School of Chemistry and Chemical Engineering, Beijing Institute of Technology, Beijing 102488, PR China
[d] College of Materials and Chemical Engineering, Hezhou University, Hezhou 542899, PR China

ARTICLE INFO

*Keywords:*
Ratiometric
Fluorescent probe
$Cu^{2+}$
Boranil derivatives

ABSTRACT

A novel ratiometric fluorescent probe **1**, consisting of Boranil derivative as the fluorophore and picolinate as the recognition site for $Cu^{2+}$, was designed and synthesized. **1** was found to display ratiometric response while interacting with $Cu^{2+}$ by undergoing a $Cu^{2+}$-promoted hydrolysis of the picolinate moiety for the release of its precursor, **2**. We observed that **1** not only showed quick response time (within 10 min), high sensitivity (detection limit of 0.52 μM), and high selectivity for $Cu^{2+}$ over other metal ions, but also allowed us to detect $Cu^{2+}$ in a convenient way of observing fluorescence color change under a 365 nm UV lamp using naked eyes. Our study introduced the first ratiometric fluorescent probe for $Cu^{2+}$ based on Boranil derivative.

## 1. Introduction

Development of techniques for monitoring heavy and transition metal cations have attracted increasing attention in recent years [1]. Among various heavy and transition metal cations, copper ion ($Cu^{2+}$), being the third most abundant cations in human body, is playing crucial roles in physiological processes [2]. It is essential to keep an appropriate amount of $Cu^{2+}$ in order to keep regular $Cu^{2+}$-mediated processes in lives. Daily doses of $Cu^{2+}$ suggested by the National Research Council are 0.4 mg to 0.6 mg, 1.5 mg to 2.5 mg and 1.5 mg to 3.0 mg for infants, children and adults, respectively [3]. The average $Cu^{2+}$ concentration is limited from 15.7 μM to 23.6 μM in blood [4]. However, aberrant $Cu^{2+}$ levels, both deficiency and excess, can cause serious diseases. Specifically, $Cu^{2+}$ deficiency can result in anemia [5], myelopathy [6] and coronary heart disease [7], neurodegenerative diseases such as Alzheimer's [8], Parkinson's [9], Wilson's [10] and Menke's [11] are associated with excessive $Cu^{2+}$. Owing to extensive use of Cu-mediated materials in industry and agriculture, continuous discharge of $Cu^{2+}$ may cause significant environmental contaminations. For these reasons, the maximum allowable levels (MAL) of $Cu^{2+}$ in drinking water defined by World Health Organization (WHO), U.S. Environmental Protection Agency (EPA) and Administration of the People's Republic of China are 30 μM [12], 20 μM [13] and 15.7 μM [4], respectively. Due to its physiological roles as well as environmental concerns, it is important to develop efficient methods of detecting $Cu^{2+}$ in biological and environmental systems.

Up to now, many conventional analytical technologies have been developed to detect $Cu^{2+}$ in quantitative manner, e.g., inductively coupled plasma mass spectrometry (ICP-MS) [14], atomic absorption spectrometry (AAS) [15], atomic emission spectrometry (AES) [16] and electrochemical [17]. However, these methods normally require expensive instruments, tedious sample preparation procedures, skilled operators, long time consumption. By contrast, use of fluorescent probes offers an efficient way to detect $Cu^{2+}$ with excellent advantages, e.g., specificity, high sensitivity, simple instrumentation, easy operation, real-time monitoring with rapid response [18]. Hence, numerous $Cu^{2+}$-selective fluorescent probes have been developed [19–36,39–41]. Typically, two strategies are employed for the design of the reported $Cu^{2+}$ fluorescent probes, coordination-based and reaction-based approaches. Due to the inherent fluorescence quenching property of paramagnetic $Cu^{2+}$, coordination-based fluorescent probes [19–24] usually exhibit turn-off fluorescence signaling upon chelating with $Cu^{2+}$,

* Corresponding authors.
*E-mail addresses:* zhudongjian@iccas.ac.cn (D. Zhu), rash_yudi@163.com (A. Ren).

https://doi.org/10.1016/j.ica.2021.120438
Received 10 February 2021; Received in revised form 26 April 2021; Accepted 3 May 2021
Available online 6 May 2021

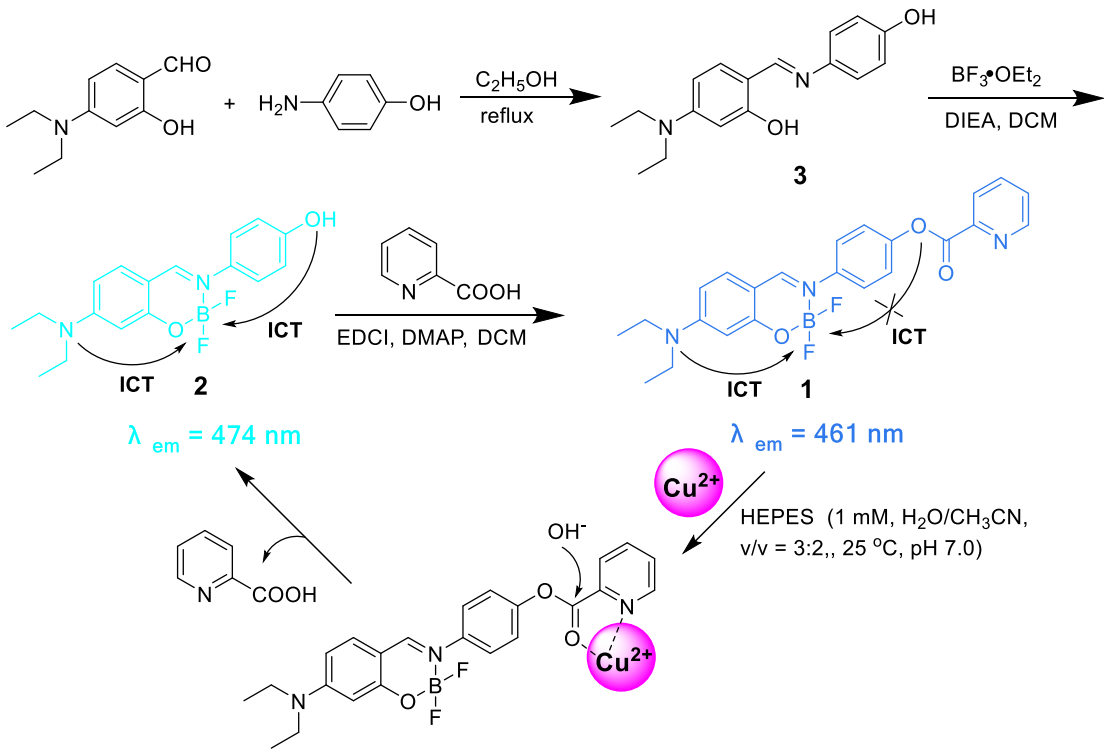


**Scheme 1.** Synthetic strategy for **1** and proposed sensing mechanism for $Cu^{2+}$.

yet may cause false-positive results. On the contrary, reaction-based strategy is an effective way to construct turn-on fluorescent probes through $Cu^{2+}$-promoted irreversible chemical reactions, including hydrolysis [25–31], oxidation [32–34], Heck [35], and Click [36] reaction. The reaction-based strategy allows for desirable fluorescence enhancement signal with high sensitivity. Actually, it is an attractive strategy to design ratiometric fluorescent probes for $Cu^{2+}$. Since intensity-based either turn-off or turn-on fluorescent probes are easily influenced by many factors, including probe concentration, instrumental efficiency, excitation intensity and environmental variations. In contrast, ratiometric fluorescent probes can eliminate most or all interferences by self-calibration of two different emission bands [37–41]. However, to the best of knowledge, only few ratiometric fluorescent probes for $Cu^{2+}$ have been reported [39–41].

It is well known that fluorescent probes generally contain two components: the fluorophore and the specific recognition site. Although different fluorophores, such as coumarin [19,28], fluorescein [22], rhodamine [21,31,34], naphthalimide [24], quinoline [23,25] and boron dipyrromethene (BODIPY) [20] have been successfully employed for the preparation of $Cu^{2+}$ fluorescent probes, fluorescent probes based on other new fluorophores are rarely reported. Thus the design and synthesis of novel fluorophores are attractive research topics in the fields of fluorescent probes recently. Boranil derivatives possess rigidify skeletons and chelate core of N^O-boron moiety, which exhibit outstanding optical properties [42,43] and can be facilely synthesized, modified and purified [44,45]. To the best of our knowledge, only two Boranil-based fluorescent probes were developed for cysteine [44] and biothiols [45] by our group, and $Cu^{2+}$-specific fluorescent probe based on Boranil derivatives has not been reported. In addition, hydrolysis reaction of the picolinate moiety has been considered as an efficient strategy for $Cu^{2+}$ fluorescent probes and receives considerable attention [25–31]. The 2-picolinic acid can be directly modified to hydroxylphenyl group of the fluorophore to yield the picolinate moiety, where the picolinate moiety can be hydrolyzed in the presence of $Cu^{2+}$ and subsequently releases the fluorophore.

With the aforementioned facts in mind, we designed and synthesized a novel fluorescent probe **1** with Boranil derivative as the fluorophore and picolinate as the recognition site for $Cu^{2+}$, as shown in Scheme 1. Boranil derivative **2** (Scheme 1) consists of electrondonating diethlyamino group and hydroxyl group, which introduces two intermolecular charge transfer (ICT) processes from diethlyamino group and hydroxyl group to the Boranil core. We reasoned that the ICT process from hydroxyl group to the Boranil core may be inhibited. We expect to see that **1** would exhibit relatively weaker fluorescence intensity and shorter emission wavelength compared to **2** (Scheme 1). When **1** mixed with $Cu^{2+}$, the ICT process from hydroxyl group to the Boranil core could be restored with an increase in fluorescence intensity and bathochromic-shift of the maximum emission wavelength. Satisfyingly, we see that first fluorescent probe based on Boranil derivatives **1** is a ratiometric fluorescent probe for sensitive and selective detection of $Cu^{2+}$.

## 2. Experimental

### 2.1. Reagents and apparatus

All the chemicals and solvents were purchased from Energy Chemical Corporation, and used as received with the following exceptions. Dichloromethane (DCM) was dried over calcium hydride. Pure water (18.25 Ω) was used to prepare all aqueous solutions. Column chromatography was conducted on silica gel (200–300 mesh). Electrospray ionization mass spectra (ESI-MS) were performed on an Agilent LC-MS 6120 equipped with Single Quadrupole LC/MS system. $^{1}H$ and $^{13}C$ nuclear magnetic resonance (NMR) spectra were recorded on Bruker Avance-400 (400 MHz) spectrometer and referenced to the residue solvent peaks (ref). UV–visible spectra were recorded in the wavelength range of 300–550 nm on a Thermo Fisher Evolution 300 UV–vis spectrometer. Fluorescence spectra were recorded in the emission wavelength range of 430–700 nm with the excitation wavelength at 405 nm using a HITACHI F-4600 spectrometer. The excitation and emission slits were set at 5 nm and 10 nm, respectively. All pH measurements were examined with a FE20 pH-Meter, and the pH values were adjusted with

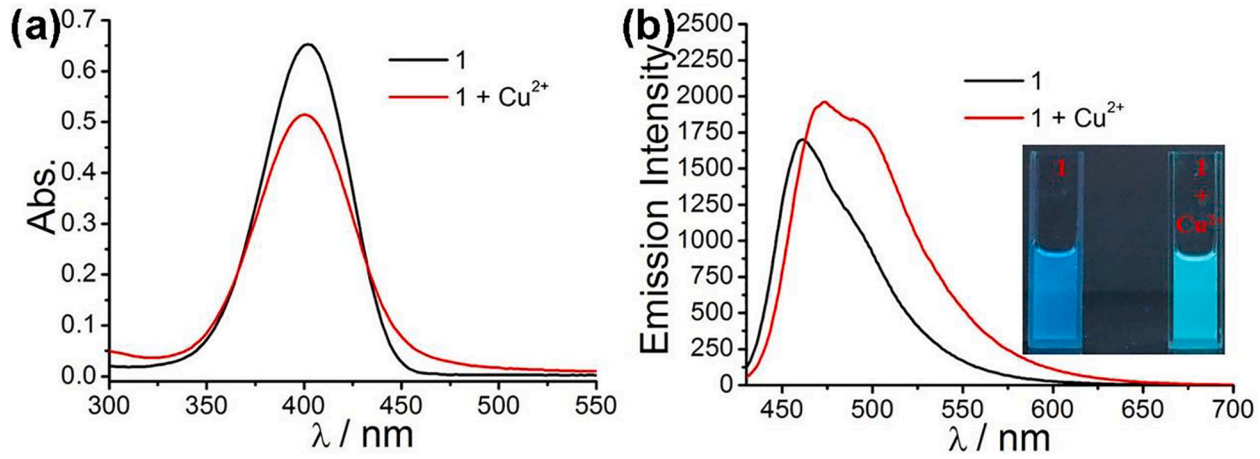


**Fig. 1.** (a) Absorption and (b) fluorescence spectra of **1** (10 μM) before (black line) and after (red line) reaction with $Cu^{2+}$ (40 μM) in HEPES buffer solution (1 mM, $H_2O/CH_3CN$, v/v = 3:2, pH 7.0, 25 °C). The fluorescence color changes of **1** before and after the reaction in HEPES buffer solution under a 365 nm UV lamp are shown in the inset.

1 M HCl and 1 N NaOH aqueous solution. The stock solution of **1** and **2** were prepared in DMSO (2 mM). The solutions of metal ions (10 mM) were prepared from commercial $CuSO_4{\cdot}5H_2O$, $Al(NO_3)_3{\cdot}9H_2O$, $BaCl_2{\cdot}2H_2O$, $CaCl_2$, $CdCl_2{\cdot}2.5H_2O$, $CoCl_2{\cdot}6H_2O$, $FeCl_3{\cdot}6H_2O$, $HgCl_2$, KCl, $MgCl_2{\cdot}6H_2O$, $MnSO_4{\cdot}H_2O$, NaCl and $ZnCl_2$. The 4-(2-hydroxyethyl)-1-piperazineethanesulfonic acid (HEPES) buffer solutions were prepared using deionized water. Fluorescence quantum yield was estimated using quinine sulfate ($\Phi_f = 0.54$ in 0.1 N $H_2SO_4$) as the reference [46].

### 2.2. Synthesis of 1

**3** and **2** were synthesized according to our previously reported method [44,45]. **2** (332.2 mg, 1.0 mmol), 2-picolinic acid (183.2 mg, 1.5 mmol), 1-ethyl-3-(3-dimethylaminopropyl)carbodiimide hydrochloride (EDCI) (287.6 mg, 1.5 mmol), and 4-dimethylaminopyridine (DMAP) (12.2 mg, 0.1 mmol) were dissolved in anhydrous DCM (30 mL) under argon atmosphere. The resulted solution was stirred overnight at room temperature. Upon completion, 0.1 M HCl aqueous solution (40 mL) was added into the reaction mixture. The mixed solution was extracted with dichloromethane (3 × 30 mL). The organic layer was combined and washed with brine, then dried over sodium sulfate. The organic solvent was evaporated to generate crude solid, which was further purified by flash chromatography (on silica gel) using DCM/methanol (100:0–100:2, v/v) as the eluent to give the desired products, 153.1 mg (35%). $^1$H NMR (400 MHz, $d_6$-DMSO, ppm) $\delta$ = 8.84–8.82 (m, 1H), 8.70 (s, 1H), 8.27 (d, $J$ = 8.0 Hz, 1H), 8.11–8.07 (m, 1H), 7.76–7.73 (m, 1H), 7.66 (d, $J$ = 8.8 Hz, 1H), 7.51 (d, $J$ = 9.2 Hz, 1H), 7.46 (d, $J$ = 9.2 Hz, 2H), 6.57–6.54 (m, 1H), 6.18 (d, $J$ = 2.0 Hz, 1H), 3.52 (q, $J$ = 7.2 Hz, 4H), 1.18 (t, $J$ = 6.8 Hz, 6H). $^{13}$C NMR (100 MHz, $d_6$-DMSO, ppm) $\delta$ = 163.4, 160.93, 159.92, 156.0, 145.0, 149.5, 146.6, 140.6, 137.7, 134.9, 127.9, 125.7, 124.1, 122.6, 106.8, 96.7, 44.4, 12.4. MS(ESI) for $C_{23}H_{23}BF_2N_3O_3^+$ ($[M + H]^+$): calcd: 438.2, found: 438.2.

## 3. Results and discussions

The synthetic route for **1** was illustrated in Scheme 1, in where **1** was made from **2** and 2-picolinic acid in the presence of EDCI and DMAP. The chemical structure of **1** was fully characterized by nuclear magnetic resonance ($^1$H NMR and $^{13}$C NMR) spectrometry and electrospray ionization (ESI-MS) mass spectrometry, which were explained in the supporting information.

The UV–vis absorption and fluorescence spectra of **1** with/without $Cu^{2+}$ in HEPES buffer solution (1 mM, $H_2O/CH_3CN$, v/v = 3:2, pH 7.0, 25 °C) were firstly evaluated. As illustrated in Fig. 1, the solution of **1** exhibited a maximum absorption peak at 402 nm with a molar extinction coefficient of 6.53 × $10^4$ L $mol^{-1}$ $cm^{-1}$. Upon adding $Cu^{2+}$, the maximum absorption peak was found to slightly bule-shift to 400 nm with a molar extinction coefficient of 5.15 × $10^4$ L $mol^{-1}$ $cm^{-1}$. When excited at 405 nm, fluorescence spectra of **1** before and after reaction with $Cu^{2+}$ displayed different fluorescence intensities and showed maximum emission peaks at 461 nm ($\Phi_f = 0.006$) and 474 nm ($\Phi_f$ = 0.085), respectively. This result is consistent with our hypothesis that ratiometric fluorescence change for the ratio of the two emission peaks at 474 nm and 461 nm ($F_{474\ nm}/F_{461\ nm}$) is observed. Simultaneously, an obvious color change from dark blue to blue was observed by naked-eyes under a 365 nm UV lamp (Fig. 1b inset). Interestingly, the absorption spectra, fluorescence spectra and fluorescence color of the reaction system are similar to those of **2** in HEPES buffer solution (Fig. S1†), indicating that the $Cu^{2+}$-promoted hydrolysis of the picolinate moiety causes the release of **2**. To further verify the proposed sensing mechanism, the mixed solution of **1** with $Cu^{2+}$ was analyzed by the ESI-MS spectrum. A major peak at $m/z$ = 333.1 $[M + H]^+$ was detected (Fig. S2†), which was consistent with the molecular weight of **2**. All these results clearly suggested that **1** underwent $Cu^{2+}$-mediated hydrolysis and released the precursor **2** (Scheme 1).

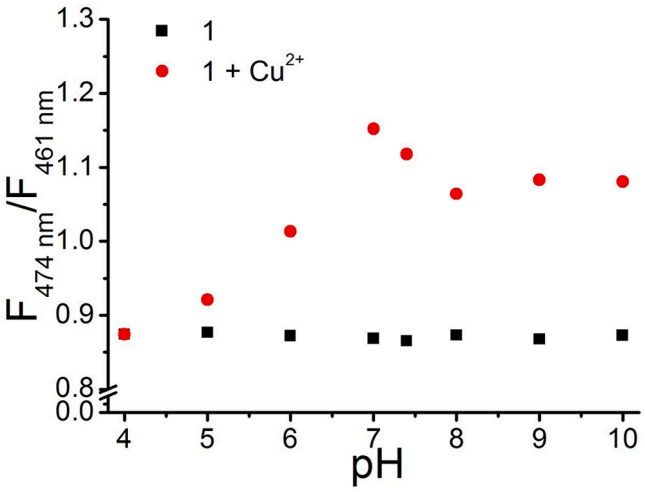


**Fig. 2.** Effect of pH on fluorescence intensity ratio of $F_{474\ nm}/F_{461\ nm}$ for **1** (10 μM) in the absence (black square) and presence (red cycle) of $Cu^{2+}$ (40 μM) in HEPES buffer solution (1 mM, $H_2O/CH_3CN$, v/v = 3:2, 25 °C, $\lambda_{ex}$ = 405 nm).

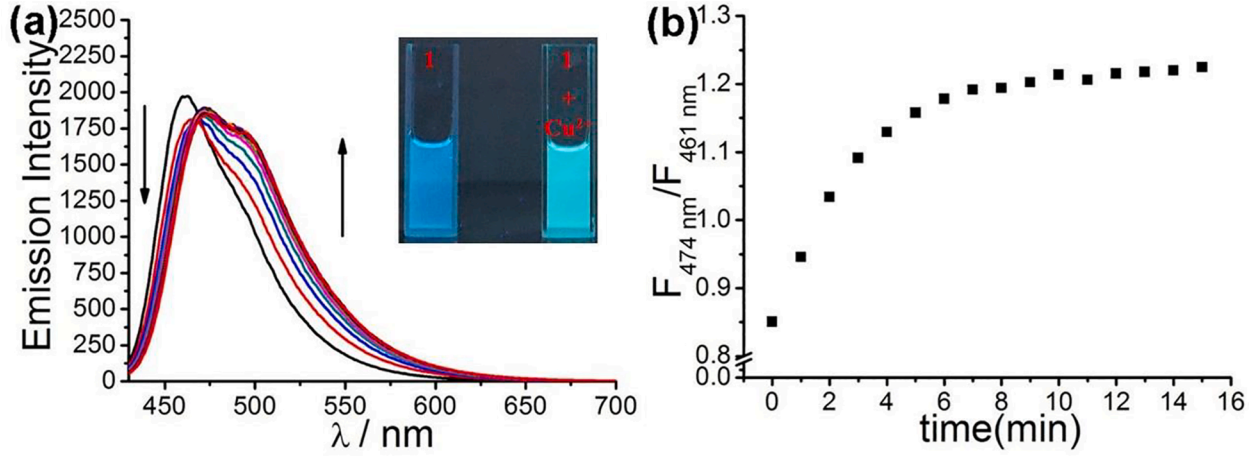


**Fig. 3.** (a) Fluorescence spectra of **1** (10 μM) recorded for 15 min in 1 min intervals after the addition of $Cu^{2+}$ (40 μM) in HEPES buffer solution (1 mM, $H_2O/CH_3CN$, v/v = 3:2, pH 7.0, 25 °C, $\lambda_{ex}$ = 405 nm). The fluorescence color changes of **1** without and with $Cu^{2+}$ in HEPES buffer solution under a 365 nm UV lamp are shown in the inset. (b) The fluorescence intensity ratio ($F_{474\ nm}/F_{461\ nm}$) changes as a function of time.

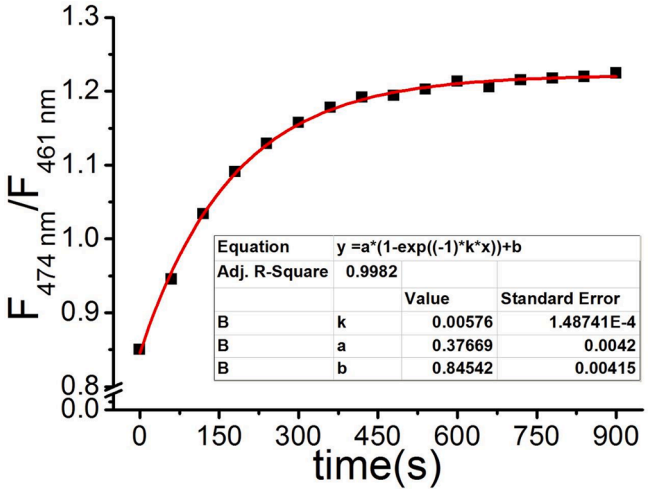


**Fig. 4.** Kinetic plot of the fluorescence intensity ratio ($F_{474\ nm}/F_{461\ nm}$) of the pseudo-first order reaction of **1** (10 μM) to $Cu^{2+}$ (40 μM), using excitation wavelength at 405 nm. The slope of the plot corresponds to the observed reaction rate of $\mathbf{5.76 \times 10^{-3}\ s^{-1}}$.

Next, we observed pH-dependent and time dependent fluorescence response upon interacting with $Cu^{2+}$. The ratios of fluorescence intensities at 474 nm and 461 nm ($F_{474\ nm}/F_{461\ nm}$) of **1** without or with $Cu^{2+}$ were explored in HEPES buffer solution (1 mM, $H_2O/CH_3CN$, v/v = 3:2, 25 °C, $\lambda_{ex}$ = 405 nm) by adjusting pH from 4.0 to 10.0 using HCl or NaOH (Fig. 2). The fluorescence intensity ratio ($F_{474\ nm}/F_{461\ nm}$) of **1** without $Cu^{2+}$ remained almost unchanged when pH changes from 4.0 to 10.0. On contrast, the fluorescence intensity ratio ($F_{474\ nm}/F_{461\ nm}$) of **1** with $Cu^{2+}$ rapidly increased in the pH range from 5.0 to 7.0 and slightly decreased in the pH range from 7.0 to 8.0. Very little change was observed in the pH range from 8.0 to 10.0. Therefore, pH 7.0 was chosen as the optimal pH in the following investigation.

Subsequently, the response time of **1** with $Cu^{2+}$ was measured by fluorescence spectroscopy in HEPES buffer solution (1 mM, $H_2O/CH_3CN$, v/v = 3:2, 25 °C, $\lambda_{ex}$ = 405 nm). As depicted in Fig. 3, the solution of **1** displayed a maximum emission peak at 461 nm (Fig. 3a). Upon addition of $Cu^{2+}$, the fluorescence intensity at 461 nm slightly decreased, and a bathochromic-shift emission peak emerged at 474 nm (Fig. 3a). Interestingly, we observed a significant color change for the solution from dark blue to blue under a 365 nm UV lamp (Fig. 3a inset), indicating that **1** can be effectively employed as an efficient ratiometric and colorimetric fluorescent probe for the detection of $Cu^{2+}$. The fluorescence intensity ratio ($F_{474\ nm}/F_{461\ nm}$) of **1** changed from 0.85 in the

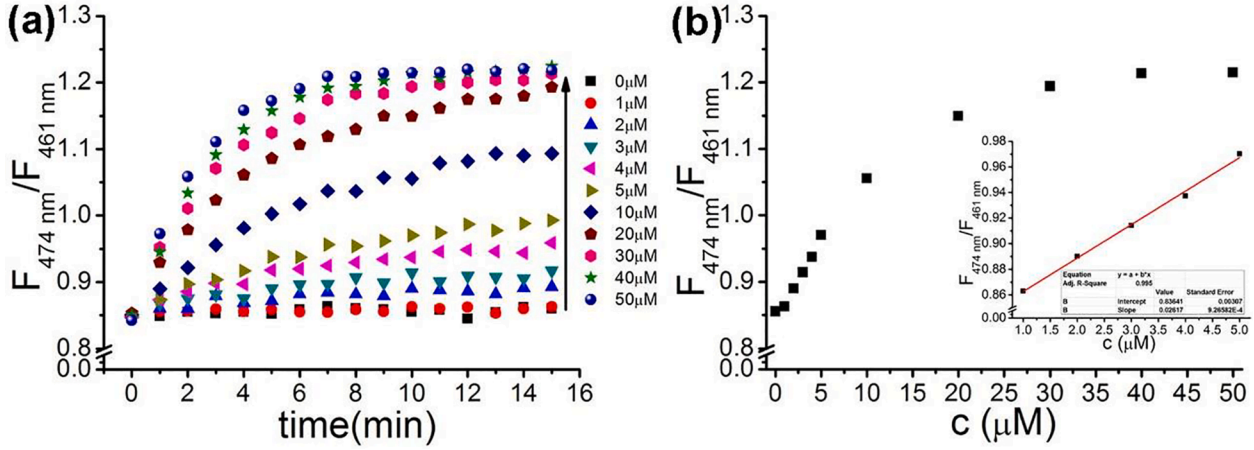


**Fig. 5.** Plot of the fluorescence intensity ratio ($F_{474\ nm}/F_{461\ nm}$) versus the response time in the presence of various concentrations of $Cu^{2+}$ (from bottom to top): 0 (control), 1 μM, 2 μM, 3 μM, 4 μM, 5 μM, 10 μM, 20 μM, 30 μM, 40 μM and 50 μM. (b) The fluorescence intensity ratio ($F_{474\ nm}/F_{461\ nm}$) as a function of $Cu^{2+}$ concentration in the range of 1–5 μM. Data were acquired in HEPES buffer solution (1 mM, $H_2O/CH_3CN$, v/v = 3:2, pH 7.0, 25 °C, $\lambda_{ex}$ = 405 nm).

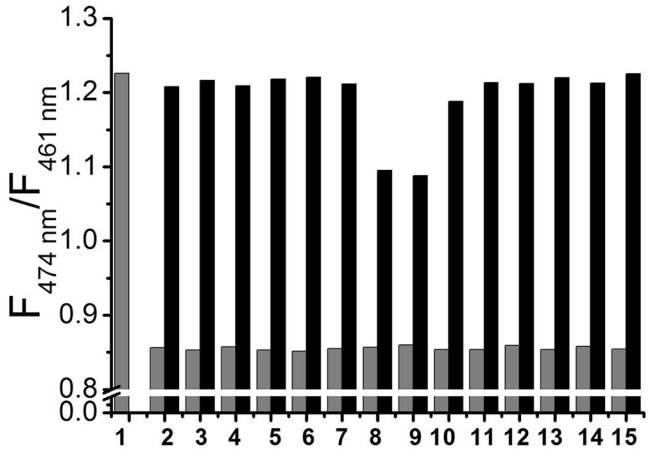


**Fig. 6.** Fluorescence responses of **1** (10 μM) to various metal ions (40 μM): 1, $Cu^{2+}$; 2, none (**1**); 3, $Ag^{+}$; 4, $Al^{3+}$; 5, $Ba^{2+}$; 6, $Ca^{2+}$; 7, $Cd^{2+}$; 8, $Co^{2+}$; 9, $Fe^{3+}$; 10, $Hg^{2+}$; 11, $K^{+}$; 12, $Mg^{2+}$; 13, $Mn^{2+}$; 14, $Na^{+}$; 15, $Zn^{2+}$. Gray bars represent the fluorescence intensity ratio ($F_{474\ nm}/F_{461\ nm}$) of **1** and **1** treated with the marked metal ions. Black bars represent the fluorescence intensity ratio ($F_{474\ nm}/F_{461\ nm}$) of **1** treated with the marked metal ions followed by $Cu^{2+}$ (40 μM). Data were acquired in HEPES buffer solution (1 mM, $H_2O/CH_3CN$, v/v = 3:2, pH 7.0, 25 °C, $\lambda_{ex}$ = 405 nm).

absence of $Cu^{2+}$ to 1.22 in the presence of $Cu^{2+}$ (Fig. 3b). In addition, the ratio of $F_{474\ nm}/F_{461\ nm}$ immediately increased in the first 5 min and reached fatigue within 10 min (Fig. 3b), suggested that the reaction of **1** and $Cu^{2+}$ can complete within 10 min. Hence the optimal response time was determined as 10 min. Moreover, kinetic measurement of the reaction between **1** (10 μM) and $Cu^{2+}$ (40 μM) under the pseudo-first-order condition gave an observed rate constant of $k_{obs} = \mathbf{5.76 \times 10^{-3}}$ $\mathbf{s^{-1}}$ (Fig. 4), indicating that **1** can be used for the real-time detection of $Cu^{2+}$ in high sensitivity.

To test sensitivity of **1** for $Cu^{2+}$, we titrated **1** with different concentrations of $Cu^{2+}$ by monitoring the fluorescence intensity ratio ($F_{474\ nm}/F_{461\ nm}$). It can be seen in Fig. 5, the fluorescence intensity ratio ($F_{474\ nm}/F_{461\ nm}$) was continuously increased while the concentration of $Cu^{2+}$ changes from 0 μM to 40 μM, and a linear relationship between the fluorescence intensity ratio ($F_{474\ nm}/F_{461\ nm}$) and $Cu^{2+}$ concentration was observed in the low concentration range of 0–5 μM (Fig. 5 inset). A linear regression curve was y = 0.83641 + 0.02617 x, with a correlation coefficient ($R^2$) of 0.995 (Fig. 5b inset). The limit of detection (LOD) of **1** to $Cu^{2+}$ was calculated to be 0.52 μM based on 3δ/k, where δ is the standard deviation of blank measurement (number of measurements = 30) and k is the slope the fluorescence intensity ratio ($F_{474\ nm}/F_{461\ nm}$) versus $Cu^{2+}$ concentration. The detection limit is much lower than the MAL of $Cu^{2+}$ in drinking water set by the WHO, U.S. EPA and Administration of the People's Republic of China. These results indicate that **1** shows high sensitivity of detecting $Cu^{2+}$ and allows for quantitative detection based on ratiometric fluorescence changes.

Besides high sensitivity, selectivity is another criteria to evaluate a fluorescent probe. The fluorescence responses of **1** toward various metal ions, including $Cu^{2+}$, $Ag^{+}$, $Al^{3+}$, $Ba^{2+}$, $Ca^{2+}$, $Cd^{2+}$, $Co^{2+}$, $Fe^{3+}$, $Hg^{2+}$, $K^{+}$, $Mg^{2+}$, $Mn^{2+}$, $Na^{+}$ and $Zn^{2+}$, were studied in HEPES buffer solution (1 mM, $H_2O/CH_3CN$, v/v = 3:2, pH 7.0, 25 °C, $\lambda_{ex}$ = 405 nm). As presented in Fig. 6 and Fig. S3†, the fluorescence intensity ratio ($F_{474\ nm}/F_{461\ nm}$) as well as fluorescence spectra of **1** induced significant changes with the addition of $Cu^{2+}$, while $Ag^{+}$, $Al^{3+}$, $Ba^{2+}$, $Ca^{2+}$, $Cd^{2+}$, $Co^{2+}$, $Fe^{3+}$, $Hg^{2+}$, $K^{+}$, $Mg^{2+}$, $Mn^{2+}$, $Na^{+}$ and $Zn^{2+}$ exhibited negligible changes in the fluorescence intensity ratio ($F_{474\ nm}/F_{461\ nm}$) and fluorescence spectra of **1**. Furthermore, the competition experiments were further explored in the presence of other metal ions mixed with $Cu^{2+}$. It can be seen that the coexistence of potentially competing other metal ions had no evident effect on the fluorescence intensity ratio ($F_{474\ nm}/F_{461\ nm}$) and fluorescence spectra of **1** to $Cu^{2+}$. The above results suggested that **1** possessed high selectivity and strong anti-interference ability for the detection of $Cu^{2+}$.

To our satisfaction, **1** can detect $Cu^{2+}$ by monitoring fluorescence color change under a 365 nm UV lamp. As demonstrated in Fig. 7, the solution of **1** mixed with $Cu^{2+}$ in the absence and presence of other metal ions ($Ag^{+}$, $Al^{3+}$, $Ba^{2+}$, $Ca^{2+}$, $Cd^{2+}$, $Co^{2+}$, $Fe^{3+}$, $Hg^{2+}$, $K^{+}$, $Mg^{2+}$, $Mn^{2+}$, $Na^{+}$ and $Zn^{2+}$), exhibited blue fluorescence, but the other aforementioned metal ions displayed dark blue fluorescence, indicating that **1** showed excellent selectivity to $Cu^{2+}$ over other metal ions.

By comparing to other fluorescent probes with picolinate as the recognition unit (Table S1), we see similar results in terms of detection limit and response time for the detection of $Cu^{2+}$. Specifically, the detection limit (0.52 μM) is similar to these of the probes based on dicyanoisophorone [29], quinolone [25], and fluorescein [47]. For the response time (10 min), it is consistent with these of fluorescent probes for $Cu^{2+}$ sensing based on BODIPY [48] and tricyanofuran [49].

## 4. Conclusion

In summary, we have developed a novel ratiometric fluorescent


**Fig. 7.** The fluorescence color changes observed before (a) and after (b) the addition of $Cu^{2+}$ (40 μM) to the solution of **1** (10 μM) in HEPES buffer solution (1 mM, $H_2O/CH_3CN$, v/v = 3:2, pH 7.0, 25 °C) under a 365 nm UV lamp in the presence of different metal ions (40 μM): $Cu^{2+}$, none (**1**), $Ag^{+}$, $Al^{3+}$, $Ba^{2+}$, $Ca^{2+}$, $Cd^{2+}$, $Co^{2+}$, $Fe^{3+}$, $Hg^{2+}$, $K^{+}$, $Mg^{2+}$, $Mn^{2+}$, $Na^{+}$, $Zn^{2+}$.

probe **1** with Boranil derivative as the fluorophore and picolinate as the recognition site. The ratiometric response was attributed to $Cu^{2+}$-assisted hydrolysis reaction of the picolinate moiety, which had been proved by absorption spectra, fluorescence spectra and ESI-MS spectrometry. **1** displayed rapid response time (within 10 min), high sensitivity (detection limit of 0.52 μM), and excellent selectivity for $Cu^{2+}$ over other metal ions. Moreover, **1** could conveniently detect $Cu^{2+}$ by fluorescence color change under a 365 nm UV lamp color changes. More importantly, **1** was the first ratiometric fluorescent probe for $Cu^{2+}$ based on Boranil derivative.

## Declaration of Competing Interest

The authors declare that they have no known competing financial interests or personal relationships that could have appeared to influence the work reported in this paper.

## Acknowledgement

This work was supported by the National Natural Science Foundation of China (21765008, 21964008), Natural Science Foundation of Guangxi (2019GXNSFDA185003, 2018GXNSFAA281166, 2020GXNSFBA159050), Students' Platform for Innovation and Entrepreneurship Training Program (201811838035), High Level Innovation Teams of Guangxi Colleges & Universities and Outstanding Scholars Program (Guijiaoren[2018]35) and Special Project on Innovation-driven Development of Hezhou (HKCPT1907006), W.Z. acknowledgements the support of the Beijing Institute of Technology Research Fund Program for Young Scholars.

## Appendix A. Supplementary data

Supplementary data to this article can be found online at https://doi.org/10.1016/j.ica.2021.120438.

## References

[1] L. Wu, C. Huang, B.P. Emery, A.C. Sedgwick, S.D. Bull, X.-P. He, H. Tian, J. Yoon, J. L. Sessler, T.D. James, Chem. Soc. Rev. 49 (2020) 5110–5139.
[2] E.L. Que, D.W. Domaille, C.J. Chang, Chem. Rev. 5 (2008) 1517–1549.
[3] Y.-H. Chan, J. Chen, Q. Liu, S.E. Wark, D.H. Son, J.D. Batteas, Anal. Chem. 82 (2010) 3671–3678.
[4] H.S. Jung, P.S. Kwon, J.W. Lee, J.I. Kim, C.S. Hong, J.W. Kim, S. Yan, J.Y. Lee, J. H. Lee, T. Joo, J.S. Kim, J. Am. Chem. Soc. 131 (2009) 2008–2012.
[5] R. Uauy, Nutr. Rev. 45 (2009) 176–180.
[6] B. Schleper, H.J. Stuerenburg, J. Neurol. 248 (2001) 705–706.
[7] A. Torrado, G.K. Walkup, B. Imperiali, J. Am. Chem. Soc. 120 (1998) 609–610.
[8] J.W. Karr, V.A. Szalai, J. Am. Chem. Soc. 129 (2007) 3796–3797.
[9] J. Li, V.N. Uversky, A.L. Fink, Biochemistry. 40 (2001) 11604–116013.
[10] L. Zhang, J. Lichtmannegger, K.H. Summer, S. Webb, I.J. Pickering, G.N. George, Biochemistry. 48 (2009) 891–897.
[11] I. Bertini, A. Rosato, Cell Mol. Life Sci. 65 (2008) 89–91.
[12] Guidelines for Drinking-water Quality. World Health Organization (WHO): Geneva, 2011.
[13] Edition of the Drinking Water Standards and Health Advisories (EPA 822-S-12-001); U.S. EPA Office of Science and Technology: Washington, 2012.
[14] J.S. Becker, A. Matusch, C. Depboylu, J. Dobrowolska, M.V. Zoriy, Anal. Chem. 79 (2007) 6074–6080.
[15] Y.E. Unsal, M. Soylak, M. Tuzen, B. Hazer, Anal. Lett. 48 (2015) 1163–1179.
[16] Y. Liu, P. Liang, L. Guo, Talanta 68 (2005) 25–30.
[17] J. Pizarro, E. Flores, V. Jimenez, T. Maldonado, C. Saitz, A. Vega, F. Godoy, R. Segura, Sens. Actuators B. 281 (2019) 115–122.
[18] M. Yang, J. Huang, J. Fan, J. Du, K. Pu, X. Peng, Chem. Soc. Rev. 49 (2020) 6800–6815.
[19] Z.-G. Wang, X.-J. Ding, Y.-Y. Huang, X.-J. Yan, B. D, Q.-Z. Li, C.-Z. Xie, J.-Y. Xu, Dyes. Pigments. 175 (2020) 108156.
[20] H.-R. Xie, Y.-Q. Gu, L. Liu, J.-C. Da, New J. Chem. 44 (2020) 19713–19722.
[21] H. Ding, B. Li, S. Pu, G. Liu, D. Jia, Y. Zhou, Sens. Actuators B. 247 (2017) 26–35.
[22] A. Panditha, K.R. Bhattarai, R.K.G. Siddappa, H.-J. Chae, Y.J. Seo, Sens. Actuators B. 282 (2019) 730–742.
[23] J. Xiong, Z. Li, J. Tan, S. Ji, J. Sun, X. Li, Y. Huo, Analyst. 143 (2018) 4870–4886.
[24] B. Guo, X. Pan, Y. Liu, L. Nie, H. Zhao, Y. Liu, J. Jing, X. Zhang, Sens. Actuators B. 256 (2018) 632–638.
[25] J. Wang, Q. Zong, Sens. Actuators B. 216 (2015) 572–577.
[26] B. Gua, L. Huang, Z. Xu, Z. Tan, M. Hu, Z. Yang, Y. Chen, C. Peng, W. Xiao, D. Yu, H. Li, Sens. Actuators B. 273 (2018) 118–125.
[27] D. Zhu, Y. Luo, X. Yan, W. Xie, W. Cai, X. Zhong, RSC Adv. 6 (2016) 87110–87114.
[28] Z. Zhou, N. Li, A. Tong, Anal. Chim. Acta 702 (2011) 81–86.
[29] R. An, D. Zhang, Y. Chen, Y. Cui, Sens. Actuators B. 222 (2016) 48–54.
[30] D. Zhu, Y. Luo, L. Shuai, W. Xie, X. Yan, Z. Duan, W. Cai, Tetrahedron Lett. 57 (2016) 5326–5329.
[31] V. Dujols, F. Ford, A.W. Czarnik, J. Am. Chem. Soc. 119 (1997) 7386–7387.
[32] J. Jo, H.Y. Lee, W. Liu, A. Olasz, C.-H. Chen, D. Lee, J. Am. Chem. Soc. 134 (2012) 16000–16007.
[33] S.S. Deshpande, S.S. Khopkar, G.S. Shankarling, Dyes Pigments. 147 (2017) 393–399.
[34] D. Ren, Y. Liu, X. Liu, Z. Li, H. Li, X.-F. Yang, Sens. Actuators B. 255 (2018) 2321–2328.
[35] Q. Wu, E.V. Anslyn, J. Am. Chem. Soc. 126 (2004) 14682–14683.
[36] B. Situ, J. Zhao, W. Lv, J. Liu, H. Li, B. Li, Z. Chai, N. Cao, L. Zheng, Sens. Actuators B. 240 (2017) 560–565.
[37] Z. Liu, G. Lia, Y. Wang, J. Li, Y. Mi, D. Zou, T. Li, Y. Wu, Talanta 192 (2019) 6–13.
[38] D. Zhu, X. Yan, A. Ren, W. Xie, Z. Duan, Anal. Chim. Acta. 1058 (2019) 136–145.
[39] S.W. Cho, A.S. Rao, S. Bhunia, Y.J. Reo, S. Singha, K.H. Ahn, Sens. Actuators B. 279 (2019) 204–212.
[40] F. Yan, Z. Bai, Y. Chen, F. Zu, X. Li, J. Xu, L. Chen, Sens. Actuators B. 275 (2018) 86–94.
[41] Z. Aydin, B. Yan, Y. Wei, M. Guo, Chem. Commun. 56 (2020) 6043–6046.
[42] D. Frath, S. Azizi, G. Ulrich, P. Retailleau, R. Ziessel, Org. Lett. 13 (2011) 3414–3417.
[43] D. Frath, S. Azizi, G. Ulrich, R. Ziessel, Org. Lett. 14 (2012) 4774–7747.
[44] D. Zhu, X. Yan, A. Ren, W. Cai, Z. Duan, Y. Luo, Anal. Methods. 11 (2019) 2579–2584.
[45] A. Ren, D. Zhu, Y. Luo, M., J. Mol. Struct. 1209 (2020), 127914.
[46] G.A. Crosby, J.N. Demas, J. Phy. Chem. 75 (1971) 991–1024.
[47] R.M. Kierat, R. Krämer, Bioorg. Med. Chem. Lett. 15 (2005) 4824–4827.
[48] C. Zhao, P. Feng, J. Cao, X. Wang, Y. Yang, Y. Zhang, J. Zhang, Y. Zhang, Org. Biomol. Chem. 10 (2012) 3104–3109.
[49] K.H. Nguyen, Y. Hao, K. Zeng, X. Wei, S. Yuan, F. Li, S. Fan, M. Xu, Y.-N. Liu, J. Photoch. Photobio. A. 358 (2018) 201–206.